

Introduction

One of the most common methods to suppress electromagnetic interference (EMI) is to use filter capacitors and inductors. This article explores how to manage radiated EMI by discussing the impedance characteristics and design methodology of these filtering components in a dual active bridge converter.

Radiated EMI Model of a Dual Active Bridge Converter

Figure 1 shows the topology and physical diagram of a dual active bridge converter, where the input and output each have a cable. The converter's input and output lines are equivalent to a pair of dipole antennas. This high-frequency common-mode (CM) voltage triggers a high-frequency CM current (I_A) on the input and output lines, and then radiates energy outward in the form of an electromagnetic field.

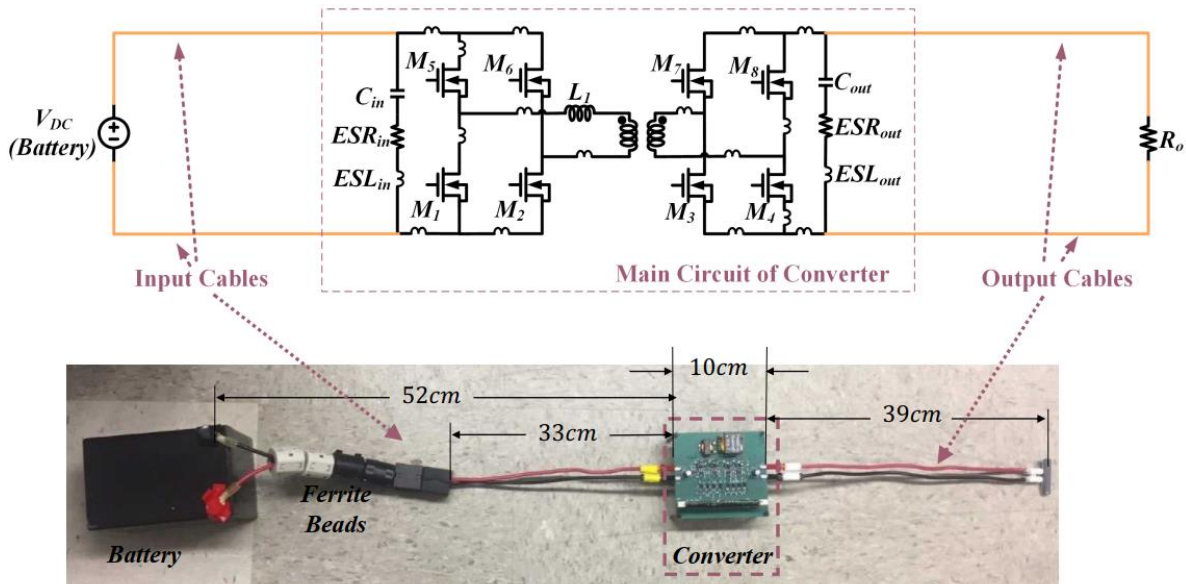
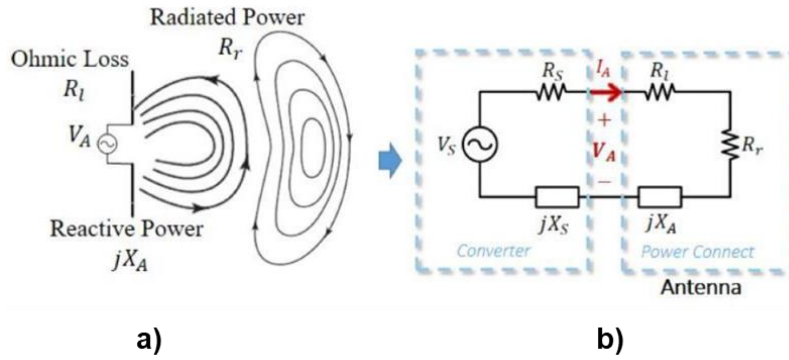


Figure 1: Topology and Physical Diagram of a Dual Active Bridge Converter

Figure 2 shows radiated EMI principles, with Figure 2a on the left showing the dipole antenna's radiation principles, and Figure 2b on the right showing the general radiated EMI model.

Figure 2a shows that the antenna's energy flows into three different parts. One part is resonated between the two poles and does not radiate into space, where jX_A is the impedance corresponding to the reactive power. The second part of the power is radiated into space, which is modelled with R_r . The last part of the energy is dissipated on the antenna's resistance, which is modelled with R_i .

Figure 2b shows a general radiated EMI model. The converter can be modeled by an equivalent noise source (V_S) and source impedance (represented by the real part, R_S , and imaginary part, X_S).



a) Radiation Principle of a Dipole Antenna
b) Radiated EMI Model of a Converter

Figure 2: Radiated EMI Principles

The CM current (I_A) amplitude ($|I_A|$) can be calculated with Equation (1):

$$|I_A| = |V_S| \times \sqrt{\frac{1}{(R_S+R_A)^2+(X_S+X_A)^2}} = |V_S| \times K_I \quad (1)$$

Where R_A is the sum of R_I and R_r , and the current coefficient (K_I) is a coefficient that is proportional to I_A .

To determine the radiated EMI, the electromagnetic field intensity generated by the converter at a set distance is measured. Consider the electric field where the maximum value of the electric field intensity (E_{MAX}) at the converter’s distance (r) can be estimated with Equation (2):

$$E_{MAX} = \sqrt{\frac{\eta D}{4\pi r^2} \frac{R_r}{R_A}} \times |V_S| \times \sqrt{\frac{R_A}{(R_S+R_A)^2+(X_S+X_A)^2}} = \sqrt{\frac{\eta D}{4\pi r^2} \frac{R_r}{R_A}} \times |V_S| \times K_E \quad (2)$$

Where η is the wave impedance, and D is the directionality. The radius (r) is the ratio of the maximum power density in that direction (D) compared to the average power density of a sphere, and the electric field intensity coefficient (K_E) is a coefficient that is directly proportional to the radiated electric field intensity.

The impedances of the antenna and the converter can be obtained through testing. For more information, refer to [Part I](#), [Part II](#), and [Part III](#) of our Measuring High-Frequency, CM Current, Voltage, and Impedance article series.

Causes of Radiated EMI Spikes

K_I can be calculated with Equation (3):

$$K_I = \sqrt{\frac{1}{(R_S+R_A)^2+(X_S+X_A)^2}} \quad (3)$$

K_E can be calculated with Equation (4):

$$K_E = \sqrt{\frac{R_A}{(R_S+R_A)^2+(X_S+X_A)^2}} \quad (4)$$

Since X_S and X_A may be both capacitive and inductive, they can cancel each other out. If the sum of R_S and R_A is small, a peak is observed on the spectrum.

Figure 3 shows the measurement results of the dual active bridge converter’s source impedance and antenna impedance. The X_S and X_A curves intersect four times. X_S and X_A can cancel out each other only when they are in opposite phases (at positions 1 and 2 in Figure 3). Additionally, as R_A at position 2 is very large (nearly 1000Ω), it is unlikely that a resonance spike occurs at this point. In contrast, R_A at position 1 is only about 100Ω (the frequency at position 1 is approximately 167MHz).

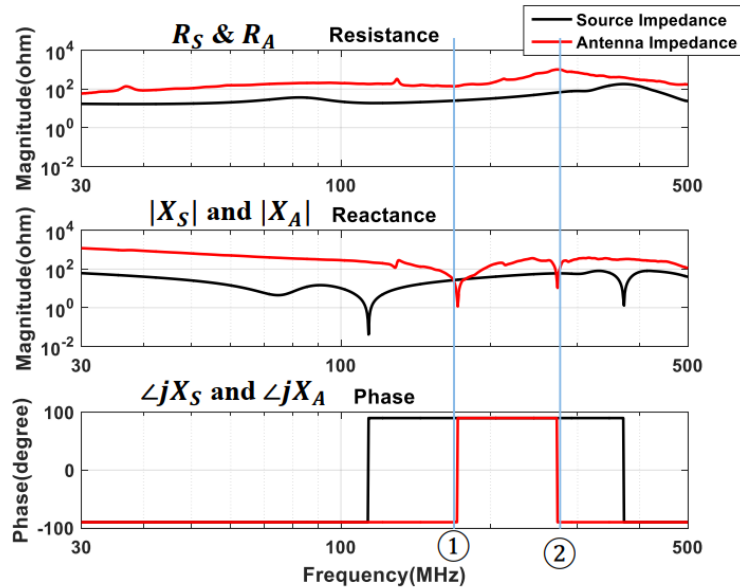


Figure 3: Source Impedance and Antenna Impedance of Dual Active Bridge Converter

Figure 4 shows the K_I and K_E curves.

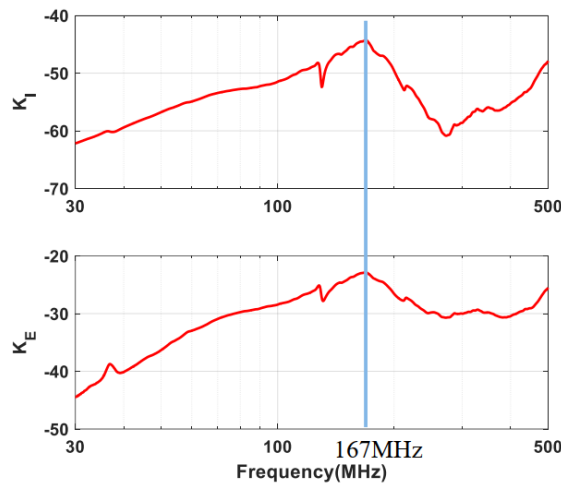


Figure 4: K_I and K_E Calculations

Figure 5 shows the spectrum of the measured I_A and the radiated EMI.

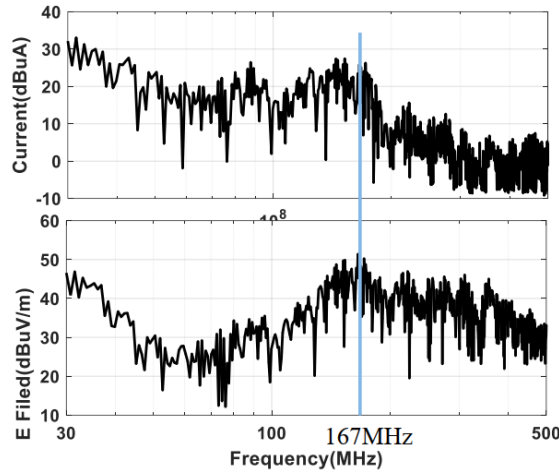


Figure 5: Measured CM Current and Radiated EMI Spectrum

At 167MHz, a resonance spike is observed due to X_S and X_A canceling out each other, and $R_S + R_A$ is small. The experimental results can also verify these results.

Impact and Design Methodology of the CM Inductor on Radiated EMI

Adding a CM inductor at the input or output terminals is a popular method to suppress radiated EMI. The inductor’s high-frequency model must typically consider the influence of its equivalent capacitance (C_P) and equivalent resistance (R_P) (see Figure 6).

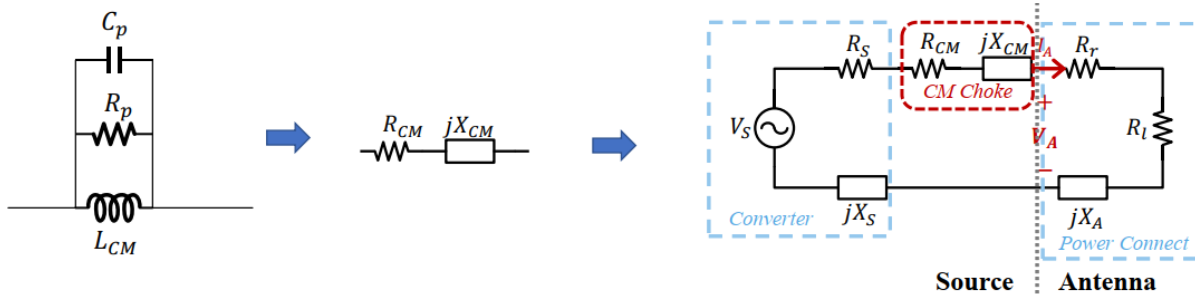


Figure 6: CM Inductance and Radiation Model Considering Inductance

To simplify the radiation model, the inductor model can be expressed as a series form of resistance (R_{CM}) and reactance (X_{CM}). By applying the inductor model to the model shown in Figure 2b, we can obtain the CM inductance and radiation model in Figure 6. It should be noted that both R_{CM} and X_{CM} change with frequency. In this case, K_I and K_E from Equation (3) and (4) must be modified to calculate for the CM current coefficient (K_{I_CM}) and CM electric field intensity coefficient (K_{E_CM}).

K_{I_CM} can be calculated with Equation (5):

$$K_{I_CM} = \sqrt{\frac{1}{(R_S + R_A + R_{CM})^2 + (X_S + X_A + X_{CM})^2}} \quad (5)$$

K_{E_CM} can be calculated with Equation (6):

$$K_{E_CM} = \sqrt{\frac{R_A}{(R_S + R_A + R_{CM})^2 + (X_S + X_A + X_{CM})^2}} \quad (6)$$

The CM inductor has three effects on radiation:

1. The resonance frequency in the radiated EMI spectrum shifts.
2. The resistance ($R_S + R_A + R_{CM}$) in the coefficients increases.
3. The reactance ($X_S + X_A + X_{CM}$) in the coefficients varies.

Reactance and resistance are analyzed separately in further detail below.

Inductor Reactance

The reactance of an inductor can be positive or negative. An inductor demonstrates inductive behavior (X_{CM} is positive) when it is below its self-resonant frequency (f_{CM}), and it demonstrates capacitive behavior when it is above f_{CM} (X_{CM} is negative). f_{CM} can be estimated with Equation (7):

$$f_{CM} = \frac{1}{2\pi\sqrt{L_{CM}C_P}} \quad (7)$$

Consider X_{CM} at the original resonance frequency (167MHz). If X_{CM} is negative (capacitive), the new resonance frequency increases; if X_{CM} is positive (inductive), the new resonance frequency decreases. Since the magnitude (V_S) typically decreases as the frequency increases, it is recommended to increase the resonance frequency so that the radiated current at this frequency can be small. Thus, proper inductor selection is important to ensure that X_{CM} is negative at the original resonance frequency.

It is also important to prevent a new resonance spike with the addition of an inductor. As the antenna impedance (X_A) is capacitive and X_{CM} remains inductive when the resonance frequency is below f_{CM} , X_{CM} must be smaller than X_A to avoid impedance crossover and the resulting resonance spike.

Inductor Resistance

R_{CM} is at its maximum value at f_{CM} . To avoid spikes, select an inductor that ensures f_{CM} is as close to the new resonance frequency as possible.

Figure 7 shows the impedance curve of a CM inductor that meets the above criteria.

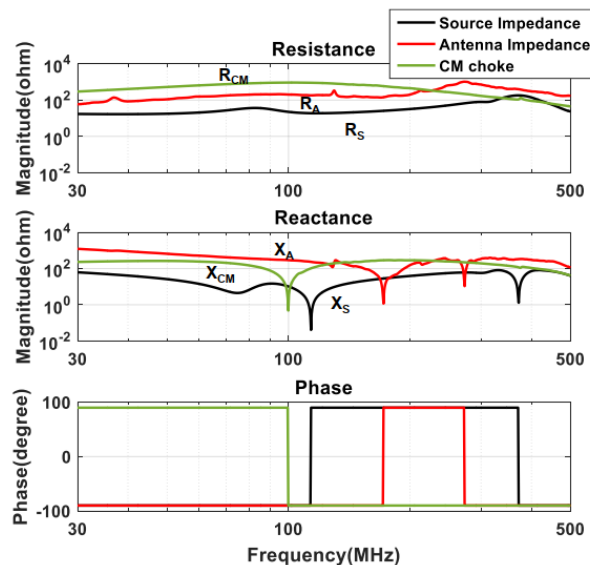


Figure 7: Impedance Curve of a CM Inductor

Figure 8 compares the K_I and K_E curves before and after adding a CM inductor. The CM inductor reduces K_I and K_E by about 13dB.

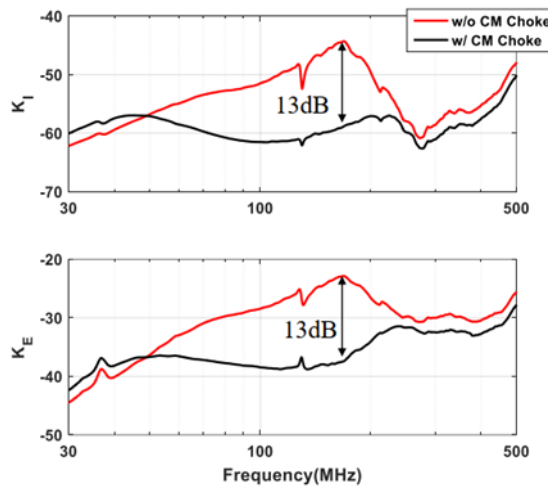


Figure 8: Comparison of K_I and K_E with or without CM Inductors

Figure 9 shows the test results of I_A (on the left) and radiated EMI (on the right) both with and without a CM inductor in the circuit.

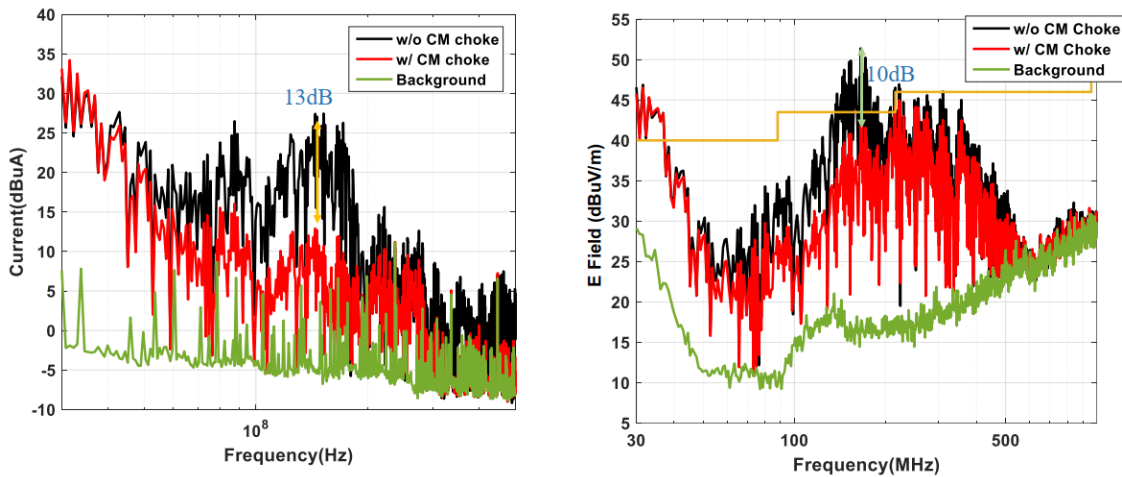


Figure 9: Comparison of CM Current and Radiated EMI with and without a CM Inductor

These results indicate that adding a CM inductor can suppress the previous spikes in EMI. The actual results are also aligned with the K_I and K_E variations. After adding a CM inductor, the noise at 167MHz meets the FCC Class B radiated EMI standard, but the margin is small. At 30MHz, the noise remains above the standard.

Impact and Design Methodology when Using a Y-Capacitor for Radiated EMI

Other filter components for suppression can be considered, such as a Y-capacitor. Connecting a Y-capacitor across the input and output DC buses is another popular method to suppress EMI. Similar to the inductor model, the Y-capacitor model can be expressed as a series form of equivalent series resistance (ESR, represented as R_Y) and reactance (X_Y) (see Figure 10).

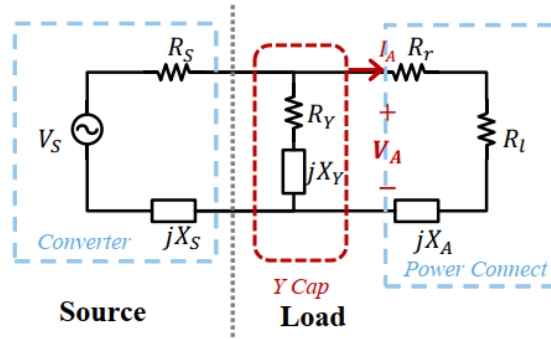


Figure 10: Radiated EMI Model Considering Y-Capacitance

In general, the Y-capacitor's R_Y is negligible and can be ignored. In addition, EMI noise can only be bypassed when the Y-capacitor's impedance is significantly smaller than the antenna impedance. Thus, we can assume that $X_Y \ll X_A$. Under these assumptions, the modified current coefficient (K_{I_Y}) and electric field intensity coefficient (K_{E_Y}) can be obtained.

K_{I_Y} can be calculated with Equation (8):

$$K_{I_Y} = \frac{|X_Y|}{\sqrt{(R_S)^2 + (X_S + X_Y)^2}} \times \frac{1}{\sqrt{R_A^2 + X_A^2}} \quad (8)$$

K_{E_Y} can be calculated with Equation (9):

$$K_{E_Y} = \frac{|X_Y|}{\sqrt{(R_S)^2 + (X_S + X_Y)^2}} \times \frac{\sqrt{R_A}}{\sqrt{R_A^2 + X_A^2}} \quad (9)$$

EMI Reduction at 30MHz and 167MHz

Due to the need to further suppress EMI noise at 30MHz and 167MHz, analysis can be conducted under these two frequency bands.

Based on the impedance curve in Figure 3, $X_A \gg R_A$, X_S , and R_S at 30MHz. By comparing K_{I_Y} and K_I (or K_{E_Y} as can be observed from K_E), the insertion loss of the Y-capacitor is calculated with Equation (10):

$$\text{Insertion Loss (30MHz)} = \frac{K_{I_Y}}{K_I} = \frac{K_{E_Y}}{K_E} \approx \frac{|X_Y|}{\sqrt{(R_S)^2 + (X_S + X_Y)^2}} \quad (10)$$

To effectively suppress EMI, the insertion loss must be below 1, where a smaller value indicates a better effect on EMI. This means that $|X_Y|$ must be below $|X_S|$, and $|X_Y|$ must be as small as possible. According to the measurements in Figure 3, if X_Y is capacitive at 30MHz, its capacitance must exceed 86pF to ensure that the insertion loss is below 1; if X_Y is inductive at 30MHz, its inductance must be below 327nH to ensure that the insertion loss is below 1.

At 167MHz, the impedance curve indicates that $R_A \gg X_A$, X_S , and R_S . Through simplification, insertion loss is consistent with Equation (10). A similar analysis indicates that if X_Y is capacitive at 167MHz, its capacitance should exceed 30pF; if X_Y is inductive at 167MHz, its inductance should be below 30nH.

Figure 11 shows two feasible Y-capacitors and their impedance curves by combining the requirements for both frequency bands. The blue curves on the left show a 100pF Y-capacitor, while the black curves on the right show a 470pF Y-capacitor. At 30MHz, the 470pF capacitor has a lower impedance, which is better for EMI suppression. At 167MHz, the 100pF capacitor demonstrates better performance.

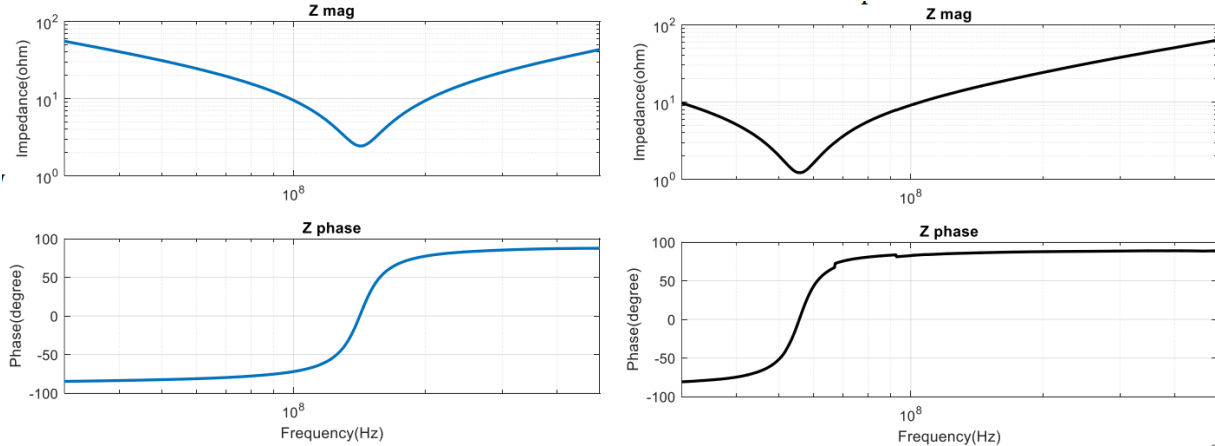
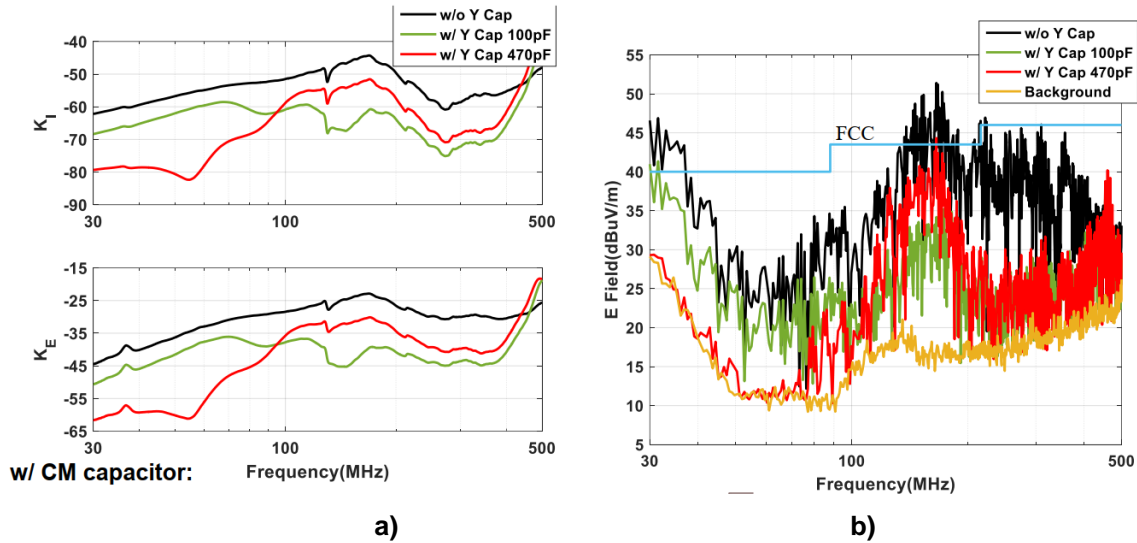


Figure 11: Impedance of Y-Capacitor at 100pF (Blue) and 470pF (Black)

Figure 12a shows a comparison of the effects of different Y-capacitors on the K_I and K_E coefficients. Both the 100pF and 470pF Y-capacitors can effectively suppress EMI. Moreover, the 100pF capacitor has a significant effect in the 167MHz frequency band, while the 470pF capacitor is more effective in the 30MHz frequency band. This is also consistent with the previous theoretical analysis.

Figure 12b shows the EMI measurement results that further validate the theoretical analysis. When using different Y-capacitors, the radiated EMI decreases to varying degrees in different frequency bands, and this reduction is consistent with the predicted results. From these results, it can be seen that for the design of radiated EMI, the filtering element can be adjusted to suppress a specific frequency band.



a) Comparison of K_I and K_E with and without Y-Capacitors
 b) Comparison of Radiated EMI with and without Y-Capacitors

Figure 12: Comparing K_I , K_E , and Radiated EMI

Principles of LC Filter Design

When both the inductor and capacitor filter components are present in the circuit (see Figure 13), the design should follow the impedance mismatch principle. If the source impedance is small, use a filter inductor with a large impedance in series; if the load impedance is large, connect a bypass capacitor with a small impedance in parallel.

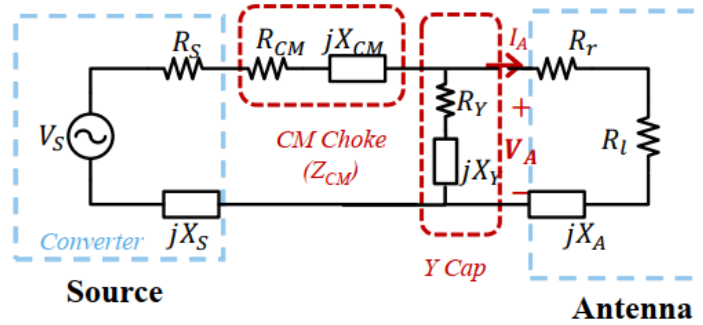


Figure 13: Radiated EMI Model with both the Inductor and Capacitor as Filter Components

Conclusion

This article reviewed the basic model of radiated EMI and introduced the principle of generating radiated EMI spikes. Then we considered a dual active bridge converter to observe how CM noise can be impacted by the CM inductor and Y-capacitor.

In the conduction frequency band, the low-frequency characteristics of the filter elements are typically used to suppress EMI. In the radiation frequency band, the stray parameters of the filter elements are typically used to achieve EMI suppression more effectively.

MPS offers a complete line of [isolation solutions](#) that are optimized for demanding industrial and automotive environments. Using capacitive isolation, MPS's isolated products minimize supply current and achieve high CMTI as well as high immunity to magnetic noise.